



Published in final edited form as:

Chem Commun (Camb). 2014 May 30; 50(42): 5604–5607. doi:10.1039/c4cc01689k.

Semiconducting polymer dots with monofunctional groups†

Fangmao Ye, Changfeng Wu‡, Wei Sun, Jiangbo Yu, Xuanjun Zhang§, Yu Rong, Yue Zhang, I-Che Wu, Yang-Hsiang Chan¶, and Daniel T. Chiu

Department of Chemistry, University of Washington, Seattle, Washington 98195, USA

Abstract

This communication describes an approach for preparing monovalent semiconducting polymer dots (mPdots) with a size of 5 nm where each mPdot was composed of precisely a single active functional group.

Monovalent fluorescent probes with sizes less than 10 nm are desirable for *in vitro* and *in vivo* biological applications.¹ Although conventional organic dyes have nanometer sizes and monovalency, they usually suffer from low absorptivity and poor photostability. These drawbacks have limited their application in high-sensitivity imaging techniques and high-throughput assays. Semiconducting quantum dots (Qdots) have been developed as brighter and more photostable probes than conventional organic dyes, but their relatively large hydrodynamic diameter and multivalency are critical constraints for biological applications.² Multivalency of Qdots may result in the cross-linking of surface proteins, which can activate signaling pathways and dramatically reduce receptor mobility. As a result, much effort has been devoted in the past several years to develop monovalent Qdots with smaller sizes.³

Semiconducting polymer dots (Pdots) have recently emerged as a new group of fluorescent probes which possess large absorption cross-sections, high quantum yields, and fast emission rates.⁴ The brightness of Pdots has been shown to be an order of magnitude higher than that of Qdots (*e.g.* 30 times) of comparable dimensions.^{4*c,i*} Moreover, several reports⁵ showed that Pdots were nontoxic to cells, an important advantage over Qdots, which can be toxic if heavy metal ions leak from the inorganic core.⁶ Finally, Pdots with sizes comparable to typical water-soluble Qdots (~15 nm) do not blink, which is an important feature in many single-molecule experiments.

These properties of Pdots make them excellent fluorescent probes for many biological applications. For example, they recently have been used for biological detection,^{4*i*} biosensing platforms,⁷ specific cellular^{4*i*} and subcellular targeting and imaging,⁸ bioorthogonal labelling,^{4*j*} protein detection^{4*b*} and *in vivo* tumor targeting.⁹ To further

†Electronic supplementary information (ESI) available: Materials, characterization and Pdots preparation. See DOI: 10.1039/c4cc01689k

Correspondence to: Daniel T. Chiu.

‡Present address: State Key Laboratory on Integrated Optoelectronics, College of Electronic Science and Engineering, Jilin University, Changchun, Jilin 130012, China.

§Present address: Division of Molecular Surface Physics & Nanoscience, Department of Physics, Chemistry, and Biology, Linköping University, Linköping 58183, Sweden.

¶Present address: Department of Chemistry, National Sun Yat-Sen University, Kaohsiung, Taiwan.

optimize Pdots for biological applications, the development of small and monovalent Pdots is the next critical step. Monovalent Pdots (mPdots) have significant advantages over conventional multivalent Pdots because a single functional group is desirable for biological applications that are sensitive to protein–nanoparticle clustering and aggregation. For example, we reported a technique for counting protein copy numbers in synaptic vesicles and subcellular organelles¹⁰ using fluorescent antibodies and single-molecule counting. For these applications, it is imperative that the fluorescent labels do not have excess functional groups that may cause cross-linking and accumulate multiple antibodies per fluorescent label.

Additionally, small Pdots (<10 nm in diameter) are desirable for certain applications. For example, we have recently developed two types of small Pdots (~9 nm), a compact yellow emitting CN-PPV Pdot⁸ and a cross-linked Pdot.¹¹ We found that these small Pdots were able to label subcellular features more efficiently than larger Pdots (~15 nm). For example, microtubules labelled with large Pdots tend to appear spotty in a confocal fluorescence image,⁴ⁱ while those same microtubules appear crisp and resolved when labelled with small Pdots.^{8,11} Small Pdots are also less prone than large Pdots to alter the diffusional and biological activity of the biomolecules that they label, and small Pdots can access size-restricted cellular regions, such as synapses. To meet these demands for the next generation of Pdots with monovalent functional groups and small size, this communication describes an approach based on surface attachment and washing for generating mPdots.

The strategy we developed to prepare mPdots is shown in Fig. 1. Here, we first form Pdots that have multiple polymer chains and are multivalent. We then attach the Pdots onto the surface of silica beads using Click chemistry. Once the Pdots are attached to the bead surface *via* a functional group (*i.e.* alkyne group), we wash the bead-Pdot with THF, which causes the Pdot to unfold and the entangled chains to fall apart, leaving a single chain of polymer attached to the bead. Re-introduction of aqueous solution causes the chain to re-collapse to form a single-chain Pdot, and subsequent release of the Pdot from the bead surface results in a monovalent Pdot (ESI[†]).

To implement the above strategy, we designed and synthesized a green emitting semiconducting polymer (alkyne terminated linear poly(*p*-phenylenevinylene) derivative containing two pendent pentaphenylene groups (PPV–PPA)). The PPV–PPA polymer had only two terminating alkyne click-functional groups (Fig. S1 and S2, ESI[†]). And because there was only two alkyne groups in the initial PPV–PPA polymer chain, during the preparation process one of the two alkyne groups was used to covalently bind to the silica surface, and later converted to the terminated Si(ONa)₃ group after NaOH cleavage when single chain PPV–PPA was formed. Therefore, there is only one alkyne group left in the single chain PPV–PPA Pdot, resulting in an mPdot with a monovalent alkyne group.

Fig. 2 shows the size information for the silica beads, regular PPV–PPA Pdots, and PPV–PPA mPdots. As established by transmission electron microscopy (TEM), the silica bead

[†]Electronic supplementary information (ESI) available: Materials, characterization and Pdots preparation. See DOI: 10.1039/c4cc01689k

(SiO₂-N₃) had a diameter of ~200 nm and the regular PPV-PPA Pdot had a 32 nm diameter (Fig. 2a and b). A representative TEM image of themPdots (Fig. 2c) shows that the mean diameter was 5.4 ± 0.5 nm (from 88 mPdots measured; Fig. 2g). Atomic force microscopy (AFM) measurements reported similar results (Fig. 2f); the mean height of mPdots was 4.5 ± 0.4 nm (from 100 mPdots imaged) (Fig. 2h). DLS showed that the hydrodynamic diameter of mPdots was 7 nm (Fig. 2i). These three measurements are consistent because the lateral dimensions of the collapsed mPdot imaged using a TEM should be slightly larger than the height of the collapsed mPdot measured using an AFM. The hydrodynamic size is ~1–2 nm larger than TEM and AFM measurements as anticipated because of slight swelling of mPdots in aqueous solution. The molecular weight of PPV-PPA we synthesized was $86\,000\text{ g mol}^{-1}$. For a single chain of PPV-PPA that is fully collapsed into a Pdot with a density of $\sim 1.0\text{ g cm}^{-3}$, the resulting mPdot would have a diameter of ~6 nm, consistent with the results from both the TEM and AFM experiments.

Our PPV-PPA mPdot had a linear chain polymer with a Si(ONa)₃ group at the end of the polymer attached to the silica surface and an alkyne group at the other end. To validate that each mPdot had only a single alkyne functional group, we followed the established approach described in the literature for confirming monovalency of nanoparticles,¹² and carried out two experiments. In the first experiment, we introduced a linker with two azide groups to crosslink mPdots. Fig. 3a shows the linker (PEG7-Bis-Azide). If mPdot was monofunctional, then after crosslinking, we expect to see dumb-bell structures (Fig. 3a). If the mPdots had more than one alkyne group, then we should see aggregates of mPdots.

Indeed, regular PPV-PPA Pdots aggregated after the addition of linkers in the presence of freshly prepared copper sulfate (0.5 mM) and L-sodium ascorbate (0.2 mM) needed to initiate the click reaction. Before the addition of a linker, there was no aggregation, which indicated that the aggregation of regular Pdots was only caused by the cross-linking of Pdots triggered by multiple click reactions among the Pdots with multiple alkyne groups. In contrast, when mPdots were used for the same experiment, we observed dumb-bell features (Fig. 3c). As a control, Fig. 3b shows a typical image of mPdots when no linker was added but in the presence of 0.5 mM copper sulfate. Fig. 3d displays the populations (singular, dumb-bell, or aggregates) of mPdots we observed in the absence and presence of a linker: ~96% of mPdots was singular when no linker was present (Fig. 3b), but when a linker was added, only ~23% of mPdots remained singular and ~75% of mPdots formed dumb-bell structures (Fig. 3c). It should be noted that the percentage of dumb-bell structures (~75%) formed by mPdots is similar to that of dumb-bell structures formed by monofunctional gold^{12b,c} or silver^{12a} nanoparticles measured by TEM as reported in the literature.¹² We do not expect 100% of mPdots (or other monovalent nanoparticles) to form dumb-bell structures because of reaction kinetics and yield as well as the stoichiometry of the linker to mPdots as we will discuss in more detail below. Importantly, we observed almost no Pdot aggregates, thus confirming the absence of multivalent Pdots.

As additional control, we varied the amount of linker that we added. For the result shown in Fig. 3c where most mPdots were in dumb-bell form, the stoichiometry or the molar ratio of the linker to mPdots was ~1 : 2. When we lowered the molar ratio of the linker to mPdots to 1 : 10, or increased the molar ratio of the linker to mPdots to 10 : 1, the majority of mPdots

appeared as a single isolated Pdote (Fig. S3, ESI[†]), similar to the image shown in Fig. 3b. For a linker to mPdote ratio of 1 : 10, there was simply insufficient linker to form dumb-bell structures, leaving mPdotes as isolated nanoparticles. For a linker : mPdote ratio of 10 : 1, we also observed individual isolated mPdotes because the reaction between the free linker and mPdote was much faster than between the mPdote-linker with another mPdote; this difference in reaction kinetics resulted in mPdotes all attached to a single linker, which prevented the formation of dumb-bell structures. This set of experiments confirmed that each mPdote had only a single functional group.

Next we converted the alkyne functional group on the mPdote to a carboxylic acid group. The motivation for this experiment was two-fold. First, carboxylic acid is one of the most common functional groups used for bioconjugation. We have demonstrated its utility in our past experiments for covalently linking a wide range of biomolecules and dyes to Pdotes and transforming them into other functional groups.^{4*i*,*j*,⁷ Therefore, this experiment acted as a gateway for changing the alkyne group to other functional groups or for attachment to biomolecules. Second, we had previously demonstrated that Cu²⁺ could crosslink Pdotes with carboxyl groups because Cu²⁺ is complexed by the carboxyl groups.¹³ Monovalent carboxyl mPdotes should also form dumb-bell structures in the presence of Cu²⁺ while polyvalent Pdotes would form aggregates as we had previously demonstrated (Fig. 4a).¹³ This experiment served as another validation that mPdotes were monovalent.}

To form mPdote-COOH, we used azide-PEG-COOH to react with mPdote-alkyne *via* click cycloaddition in the presence of copper sulfate (0.5 mM) and L-sodium ascorbate (0.2 mM). Regular multivalent Pdotes had a high density of alkyne groups on the surface and quickly aggregated in the presence of copper sulfate when the alkyne groups were transformed to COOH groups (Fig. 4b). The solution turned cloudy. Under the same conditions, mPdotes did not aggregate and the solution remained clear. We then dialyzed out the remaining copper(I)/(II) in the mPdote solution and added a more concentrated Cu²⁺ solution at 10 mM to induce mPdotes to form dumb-bell structures. Fig. 4d shows the result, in which dumb-bell features can be clearly discerned. No aggregates of mPdotes were detected, even at 10 mM of Cu²⁺; we note for regular Pdotes with COOH groups that only ~5 μM of Cu²⁺ was sufficient to induce significant Pdote aggregation.¹³ Fig. 4e shows the populations of mPdotes (singular, dumb-bell, or aggregates) in the AFM images: ~94% of multivalent Pdotes was observed to form aggregates in the presence of Cu²⁺, but for mPdotes in the presence of Cu²⁺, they formed dumb-bell structures instead (60%). Some mPdotes remained singular (38%), likely because Cu²⁺ is not as strong a cross linker and the stability of two Pdotes linked by a single Cu²⁺ ion is rather low and prone to disruption. In fact, Cu²⁺ attached to a single carboxyl group is not stable and two carboxyl groups are required to form a stable complex, which also explains why having more Cu²⁺ than mPdotes in solution did not prevent formation of dumb-bell structures. From these experiments, the strong contrast in the behavior of regular multivalent Pdotes and mPdotes is evident.

Finally, we investigated the stability of mPdotes in different buffer solutions. Fig. S4 (ESI[†]) shows the normalized fluorescence intensity of mPdotes in different buffers (including TRIS, TBE, PBS and HEPES buffer) as a function of time. The result indicated that the fluorescence of the mPdotes buffer solution did not change over a period of three days.

Because any aggregation of Pdots would result in a decrease in the measured fluorescence intensity due to self-quenching,¹⁴ this result confirmed that the Pdots are well dispersed and stable over this period, which are suitable for biological applications.

In conclusion, we have developed a method for preparing monovalent and very small Pdots. We carried out two experiments to show that mPdots only had a single functional group. When the mPdots were crosslinked, they formed dumb-bell structures as seen using an AFM. We generated clickable mPdots as well as mPdots with a single carboxyl group, which could be used for covalent attachment of a broad range of biological molecules. The importance of having monovalency has been illustrated in the literature for other nanoparticles. For example, monovalent nanoparticles have been shown to label glutamate receptors at neuronal synapses without activating EphA3 tyrosine kinase^{3b} while polyvalent nanoparticles result in activation. Monovalent nanoparticles have also been shown to offer improved quantification in tumor targeting and imaging,^{3a} and better performance in the tracking of individual proteins in live cells.¹⁵ The development of the very small and monovalent mPdots, coupled with the high brightness of Pdots as we have previously demonstrated,^{4c,i} is expected to advance their adoption as useful fluorescent probes in biomedical applications.

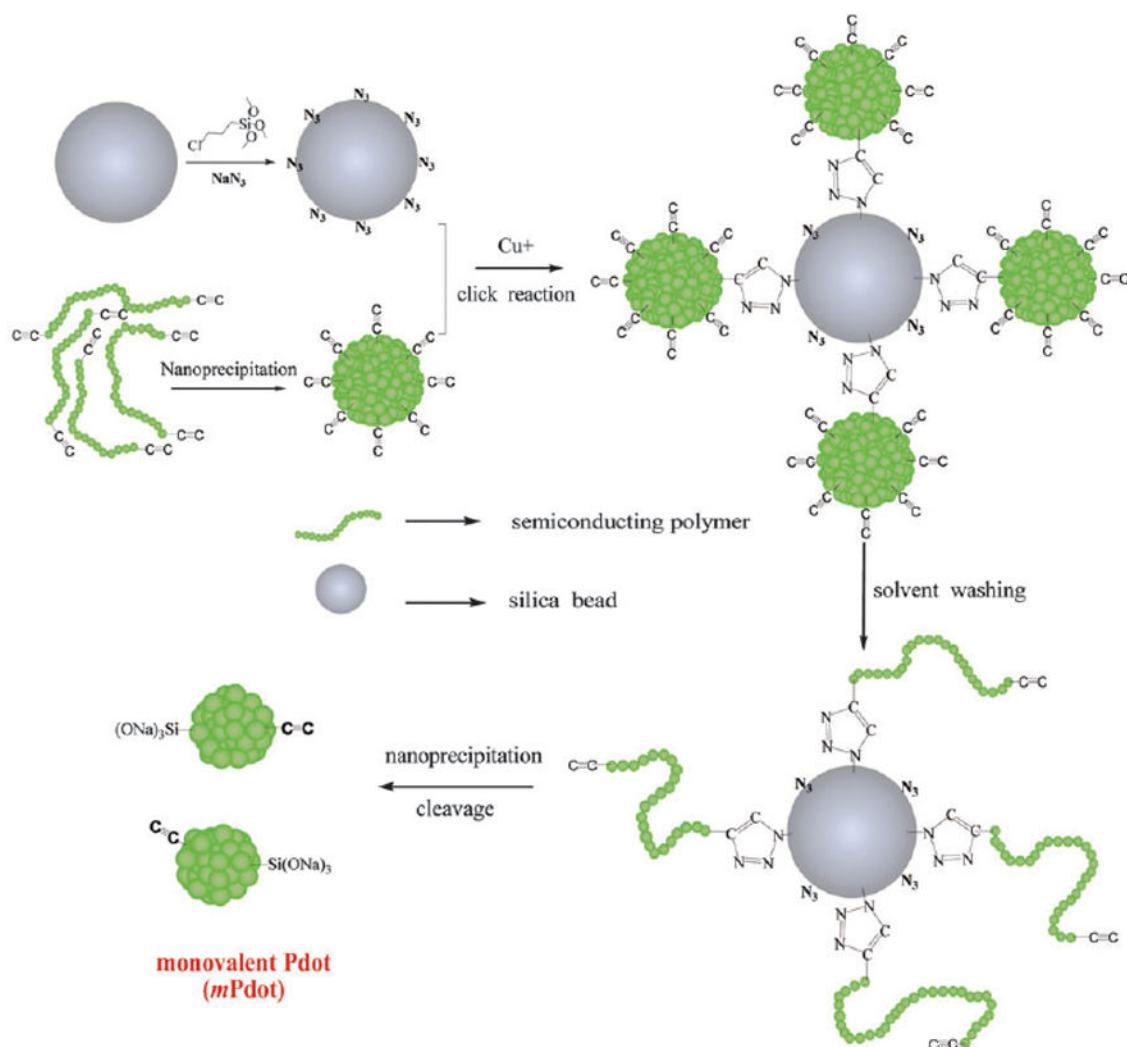
Supplementary Material

Refer to Web version on PubMed Central for supplementary material.

Notes and references

- (a) Hilderbrand SA, Kelly KA, Weissleder R, Tung C-H. *Bioconjugate Chem.* 2005; 16:1275–1281. (b) Shao F, Weissleder R, Hilderbrand SA. *Bioconjugate Chem.* 2008; 19:2487–2491. (c) Shi W, Dolai S, Rizk S, Hussain A, Tariq H, Averick S, L'Amoreaux W, ElIdrissi A, Banerjee P, Raja K. *Org Lett.* 2007; 9:5461–5464. [PubMed: 18020348] (d) Wu S, Zhu C, Zhang C, Yu Z, He W, He Y, Li Y, Wang J, Guo Z. *Inorg Chem.* 2011; 50:11847–11849. [PubMed: 22035018]
- Larson DR, Zipfel WR, Williams RM, Clark SW, Bruchez MP, Wise FW, Webb WW. *Science.* 2003; 300:1434–1436. [PubMed: 12775841]
- (a) Liu HY, Gao X. *Bioconjugate Chem.* 2011; 22:510–517. (b) Howarth M, Liu W, Puthenveetil S, Zheng Y, Marshall LF, Schmidt MM, Witttrup KD, Bawendi MG, Ting AY. *Nat Methods.* 2008; 5:397–399. [PubMed: 18425138]
- (a) Zhang X, Yu J, Rong Y, Ye F, Chiu DT, Uvdal K. *Chem Sci.* 2013; 4:2143–2151. (b) Ye F, Smith PB, Wu C, Chiu DT. *Macromol Rapid Commun.* 2013; 34:785–790. [PubMed: 23637077] (c) Wu C, Chiu DT. *Angew Chem Int Ed.* 2013; 52:3086–3109. (d) Sun W, Yu J, Deng R, Rong Y, Fujimoto B, Wu C, Zhang H, Chiu DT. *Angew Chem Int Ed.* 2013; 52:11294–11297. (e) Rong Y, Wu C, Yu J, Zhang X, Ye F, Zeigler M, Gallina ME, Wu I-C, Zhang Y, Chan Y-H. *ACS Nano.* 2013; 7:376–384. [PubMed: 23282278] (f) Zhu C, Liu L, Yang Q, Lv F, Wang S. *Chem Rev.* 2012; 112:4687–4735. [PubMed: 22670807] (g) Li K, Liu B. *J Mater Chem.* 2012; 22:1257–1264. (h) Das S, Powe AM, Baker GA, Valle B, El-Zahab B, Sintim HO, Lowry M, Fakayode SO, McCarroll ME, Patonay G, Li M, Strongin RM, Geng ML, Warner IM. *Anal Chem.* 2012; 84:597–625. [PubMed: 22050042] (i) Wu C, Schneider T, Zeigler M, Yu J, Schiro PG, Burnham DR, McNeill JD, Chiu DT. *J Am Chem Soc.* 2010; 132:15410–15417. [PubMed: 20929226] (j) Wu C, Jin Y, Schneider T, Burnham DR, Smith PB, Chiu DT. *Angew Chem Int Ed.* 2010; 49:9436–9440. (k) Pecher J, Mecking S. *Chem Rev.* 2010; 110:6260–6279. [PubMed: 20684570] (l) Wu C, Bull B, Szymanski C, Christensen K, McNeill J. *ACS Nano.* 2008; 2:2415–2423. [PubMed: 19206410]
- (a) Fernando LP, Kandel PK, Yu J, McNeill J, Ackroyd PC, Christensen KA. *Biomacromolecules.* 2010; 11:2675–2682. [PubMed: 20863132] (b) Rahim NAA, McDaniel W, Bardon K, Srinivasan S,

- Vickerman V, So PTC, Moon JH. *Adv Mater.* 2009; 21:3492–3496.(c) Pu KY, Li K, Shi JB, Liu B. *Chem Mater.* 2009; 21:3816–3822.
6. Hardman R. *Environ Health Perspect.* 2006; 114:165–172. [PubMed: 16451849]
 7. (a) Ye F, Wu C, Jin Y, Chan Y-H, Zhang X, Chiu DT. *J Am Chem Soc.* 2011; 133:8146–8149. [PubMed: 21548583] (b) Chan Y-H, Wu C, Ye F, Jin Y, Smith PB, Chiu DT. *Anal Chem.* 2011; 83:1448–1455. [PubMed: 21244093]
 8. Ye F, Wu C, Jin Y, Wang M, Chan Y-H, Yu J, Sun W, Hayden S, Chiu DT. *Chem Commun.* 2012; 48:1778–1780.
 9. Wu C, Hansen SJ, Hou Q, Yu J, Zeigler M, Jin Y, Burnham DR, McNeill JD, Olson JM, Chiu DT. *Angew Chem Int Ed.* 2010; 50:3430–3434.
 10. (a) Mutch SA, Kensel-Hammes P, Gadd JC, Fujimoto BS, Allen RW, Schiro PG, Lorenz RM, Kuyper CL, Kuo JS, Bajjalieh SM, Chiu DT. *J Neurosci.* 2011; 26:1461–1470.(b) Mutch SA, Fujimoto BS, Kuyper CL, Kuo JS, Bajjalieh SM, Chiu DT. *Biophys J.* 2007; 92:2926–2943. [PubMed: 17259276]
 11. Yu J, Wu C, Zhang X, Ye F, Gallina ME, Rong Y, Wu IC, Sun W, Chan Y-H, Chiu DT. *Adv Mater.* 2012; 24:3498–3504. [PubMed: 22684783]
 12. (a) VICKOVA B, Moskovits M, Pavel I, Siskova K, Sladkova M, Slouf M. *Chem Phys Lett.* 2008; 455:131–134.(b) Liu X, Worden JG, Dai Q, Zou J, Wang J, Huo Q. *Small.* 2006; 2:1126–1129. [PubMed: 17193575] (c) Worden JG, Dai Q, Shaffer AW, Huo Q. *Chem Mater.* 2004; 16:3746–3755.
 13. Chan Y, Jin Y, WU C, Chiu DT. *Chem Commun.* 2010; 47:2820–2822.
 14. Jin Y, Ye F, Wu C, Chan Y-H, Chiu DT. *Chem Commun.* 2012; 48:3161–3163.
 15. Clarke S, Pinaud F, Beutel O, You C, Piehler J, Dahan M. *Nano Lett.* 2010; 10:2147–2154. [PubMed: 20433164]

**Fig. 1.**

The procedure to prepare monovalent Pdots (mPdots). A silica particle with a diameter of ~200 nm was prepared and its surface modified with a layer of chloride ($\text{SiO}_2\text{-Cl}$) via the hydrolysis and condensation of chloridetriethoxysilane. The $\text{SiO}_2\text{-Cl}$ groups were then modified to azide to form a clickable silica nanoparticle (ESI^\dagger). Separately, regular multivalent PPV-PPA Pdots were prepared using nanoprecipitation (ESI^\dagger); these Pdots had alkyne groups so they could react with $\text{SiO}_2\text{-N}_3$ on the silica surface via click chemistry. Once the regular PPV-PPA Pdots were clicked onto the surface of the silica nanoparticle, the solvent was changed from aqueous solution to THF and the silica-polymer complex was washed with THF several times. This step removed all the polymer chains in the regular Pdote that were not covalently attached to the silica surface. The single polymer chains attached to the surface of the silica nanoparticles were then reprecipitated into small and monovalent mPdots by reintroducing the silica-polymer complex into aqueous solution from THF. Finally, the mPdots were cleaved from the silica surface and released into solution in the presence of NaOH and Triton 100. To remove NaOH and Triton 100, the mPdote solution was dialyzed overnight in water or buffer.

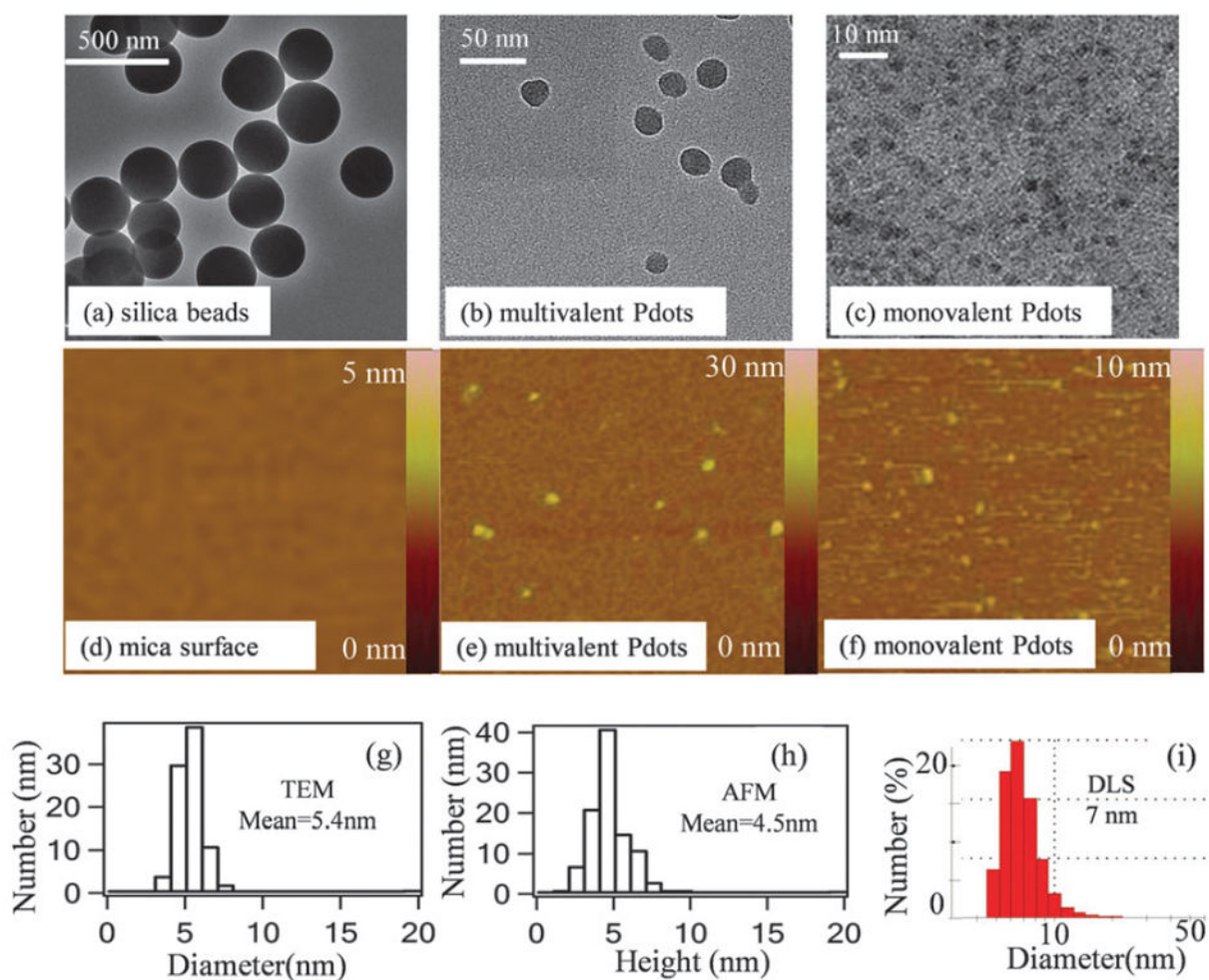


Fig. 2.

Size distribution of mPdots measured using TEM, AFM, and DLS. (a) TEM image of silica beads showing a diameter of ~ 200 nm. (b) TEM image of regular PPV-PPA Pdots, which have an average diameter of 34 ± 4 nm, from measurements on 80 Pdots. (c) TEM image of PPV-PPA mPdots. (d) AFM image ($1 \mu\text{m} \times 1 \mu\text{m}$) of the 3-aminopropyltriethoxysilane (APTEOS)-coated mica surface without any nanoparticles. (e) AFM image ($0.6 \mu\text{m} \times 0.6 \mu\text{m}$) of multivalent regular PPV-PPA Pdots. (f) AFM image ($1.2 \mu\text{m} \times 1.2 \mu\text{m}$) of PPV-PPA mPdots. (g) Size distribution of mPdots shown in (c); the average diameter was 5.4 ± 0.5 nm from images of 88 mPdots. (h) Height distribution of mPdots measured using AFM; the average value was 4.5 ± 0.4 nm from measurements on 100 mPdots. (i) DLS results of mPdots in aqueous solution showing a hydrodynamic diameter of 7 nm.

bars in (b) and (c) represent 20 nm. (d) A plot showing the populations of mPdots (singular, dumb-bell, or aggregates) observed in the AFM images in the absence and presence of linkers. About 100 Pdots were counted for calculating the percentages.

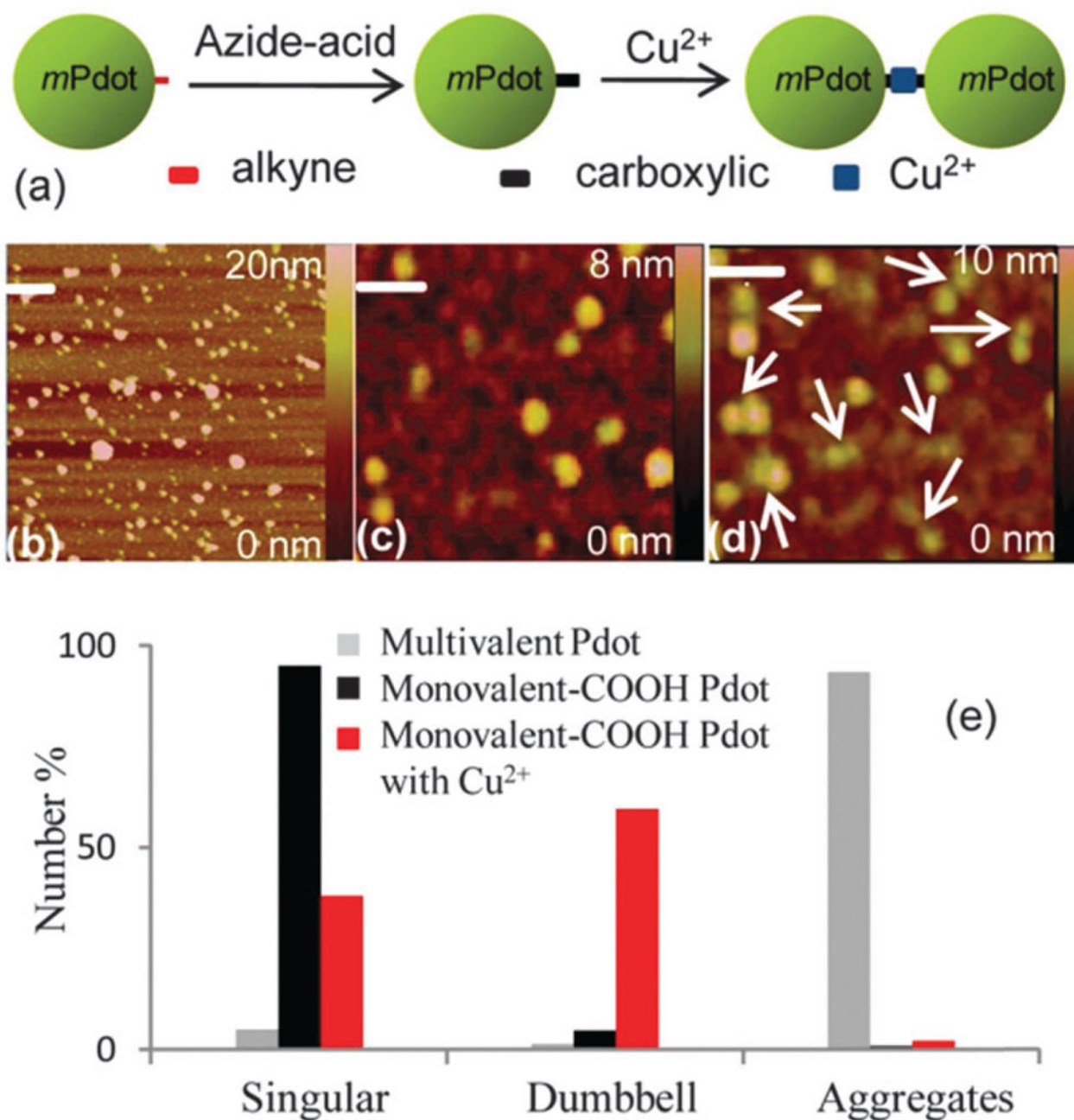


Fig. 4. Generation of carboxyl-terminated mPdots and the formation of carboxyl mPdot dumb-bells in the presence of Cu^{2+} . (a) Schematic showing the transformation of alkyne to carboxylic mPdots and then cross-linking mPdot-COOH to form dumb-bell structures. (b) AFM image of regular polyvalent carboxyl Pdots, formed from alkyne Pdots using azide-acid, in the presence of 0.5 mM Cu^{2+} in HEPES buffer ($\text{pH} = 7.4$); only aggregates were observed. (c) AFM image of mPdots with the carboxyl group in HEPES buffer ($\text{pH} = 7.4$) but without Cu^{2+} . (d) AFM image of mPdots with the carboxyl group in the presence of 10 mM Cu^{2+} in HEPES buffer ($\text{pH} = 7.4$). The white arrows point to the dumb-bell structures. Scale bars in

(b), (c), and (d) represent 100 nm, 25 nm, and 20 nm, respectively. (e) A plot showing the populations of regular multivalent Pdots and mPdots (singular, dumb-bell, or aggregates) in the AFM images in the absence and presence of Cu^{2+} . About 100 Pdots were counted for calculating the percentages.

Author Manuscript

Author Manuscript

Author Manuscript

Author Manuscript